iScience

CellPress
OPEN ACCESS

Article

Deciphering the role of endothelial granulocyte macrophage-CSF in chronic inflammation associated with HIV

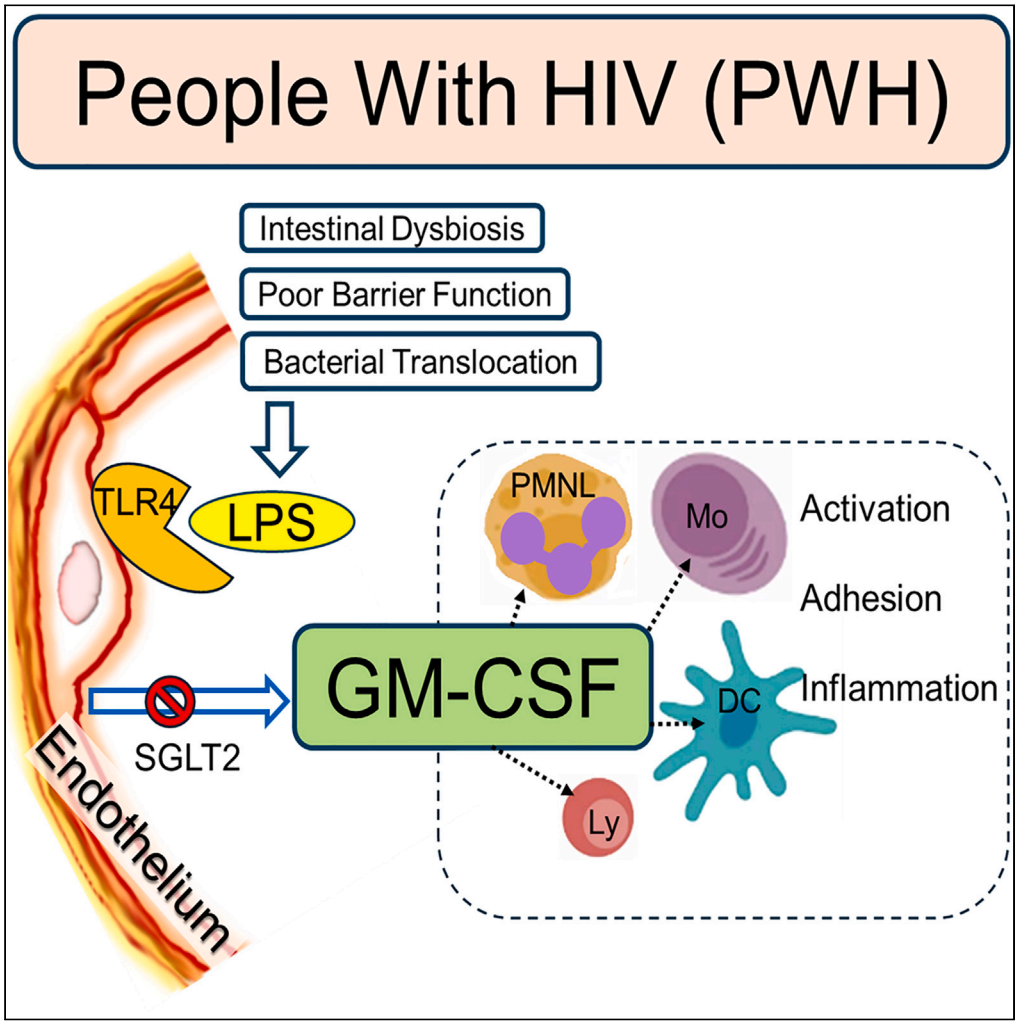

Soumya Panigrahi, Elizabeth Mayne, Susan Louw, ..., Michael M. Lederman, Michael L. Freeman, Scott F. Sieg

sxp579@case.edu

Highlights

Increased GM-CSF, TLR4, and myeloperoxidase found in the aortic endothelium of PWH

LPS triggers glucose uptake and GM-CSF expression in human endothelial cells

SGLT2 inhibitors reduce glucose uptake, GM-CSF release, and endothelial dysfunction

PWH on SGLT2 inhibitors have lower plasma GM-CSF levels than non-diabetic PWH

Panigrahi et al., iScience 27, 110909
October 18, 2024
https://doi.org/10.1016/j.isci.2024.110909

iScience

CellPress
OPEN ACCESS

Article

Deciphering the role of endothelial granulocyte macrophage-CSF in chronic inflammation associated with HIV

Soumya Panigrahi,[1,5,*] Elizabeth Mayne,[2] Susan Louw,[3] Nicholas T. Funderburg,[4] Archeesha Chakraborty,[1] Jeffrey M. Jacobson,[1] Stephen M. Carpenter,[1] Michael M. Lederman,[1] Michael L. Freeman,[1] and Scott F. Sieg[1]

SUMMARY

People with HIV (PWH) experience endothelial dysfunction (ED) that is aggravated by chronic inflammation and microbial translocation across a damaged gut barrier. Although this paradigm is well-described, downstream pathways that terminate in endothelial dysfunction are only partially understood. This study found increased expression of granulocyte macrophage colony stimulating factor (GM-CSF), toll-like receptor-4 (TLR4), and myeloperoxidase in the aortic endothelium of PWH compared to those without HIV. Bacteria-derived lipopolysaccharide (LPS) heightened glucose uptake and induced GM-CSF expression in primary human endothelial cells. Exposure to sodium-glucose cotransporter-2 (SGLT2) inhibitors reduced glucose uptake, GM-CSF release, and ED in LPS-activated endothelial cells *ex vivo*, and PWH treated with SGLT2 inhibitors for diabetes had significantly lower plasma GM-CSF levels than non-diabetic PWH not on this medication. The findings suggest that microbial products trigger glucose uptake and GM-CSF expression in the endothelium, contributing to localized inflammation in PWH. Modifying this altered state could offer therapeutic benefits.

INTRODUCTION

The vascular endothelium plays a central role in local inflammation, with activated endothelial cells (ECs) releasing pro-inflammatory mediators and growth factors including granulocyte macrophage colony stimulating factor (GM-CSF) in response to inflammatory stimuli.[1–4] GM-CSF promotes the survival, proliferation, and activation of hematopoietic progenitor cells belonging to the myeloid lineage, facilitates communication between lymphocytes and myeloid cells, and is required by myeloid cells for normal growth and differentiation.[5,6] Ongoing systemic inflammation may also directly induce endothelial dysfunction (ED),[7] typically defined by reduced bioavailability of nitric oxide (NO), an increase in endothelium-derived contracting factors, transcriptional modulation of adhesion molecules, and release of procoagulant and proinflammatory molecules that can contribute to the initiation of atherosclerotic cardiovascular disease (CVD).[8–10] ED is characterized by a reduction in the expression of endothelial cell Krüppel-like factor 2 (KLF2), a zinc finger transcription factor that regulates levels of endothelial NO synthase (eNOS), vascular cell adhesion molecule 1 (VCAM1), and E-selectin, and these ED biomarkers are important CVD monitoring tools. Moreover, ED is directly implicated in the pathogenesis of CVD in people with HIV (PWH), potentially contributing to their increased risk of CVD.[11–14]

Translocation of bacterial products from the gut lumen into the bloodstream is linked to chronic inflammation in multiple conditions including inflammatory bowel disease, cancer, chronic infectious disease, and in PWH.[13,15,16] These pathogen-associated molecular patterns (PAMPs) engage innate pattern recognition receptors to activate downstream proinflammatory signaling pathways.[17] Lipopolysaccharide (LPS), a component of the gram-negative bacterial cell wall, is a well-defined PAMP that regulates KLF2 expression to drive innate immune activation and chronic inflammation.[15] Aggregates of LPS are split into monomers by CD14 and then presented to complexes of toll-like receptor-4 (TLR4) and myeloid differentiation factor-2 (MD2) on the cell surface. This monomeric interaction is facilitated by the direct binding and presentation of LPS by LPS-binding protein (LBP).[18]

Here, we investigated a potential link between LPS and GM-CSF-associated inflammation. We hypothesized that GM-CSF expression would be elevated in the vascular endothelial tissue of PWH as a consequence of increased exposure to translocated microbial products, such as LPS. We found that manipulating endothelial glucose metabolism with an inhibitor of sodium glucose co-transporter 2 (SGLT2)

[1]Division of Infectious Diseases and HIV Medicine, Department of Medicine, Case Western Reserve University School of Medicine, Cleveland, OH, USA
[2]Division of Immunology, Department of Pathology, Faculty of Health Sciences, University of Cape Town and National Health Laboratory Service, Cape Town, South Africa
[3]Department of Molecular Medicine and Hematology, School of Pathology, Faculty of Health Sciences, and National Health Laboratory Service, University of the Witwatersrand, Johannesburg, South Africa
[4]School of Health and Rehabilitation Sciences, Ohio State University, Columbus, OH, USA
[5]Lead contact
*Correspondence: sxp579@case.edu
https://doi.org/10.1016/j.isci.2024.110909

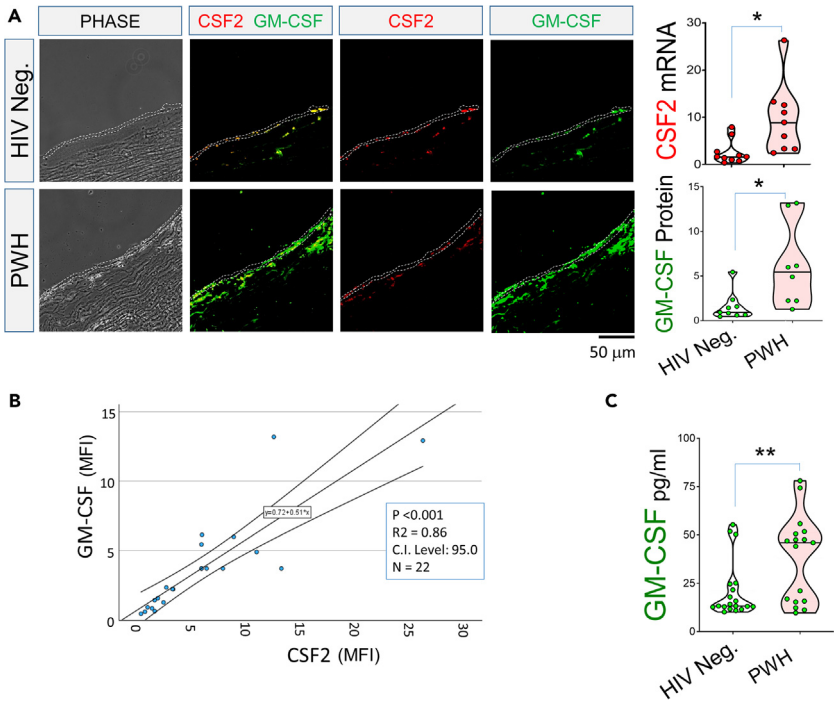

Figure 1. Dual gene expression analysis and GM-CSF protein quantification in the vascular endothelium of PWH

(A) Representative combined FISH and immunofluorescence staining in the vascular endothelium and subendothelial tissues obtained an HIV negative (top) and an PWH (bottom) donors for *CSF2* mRNA (red) and GM-CSF protein (green); the endothelial lining is shown by the space between dashed lines; each circle represents the average fluorescence intensity data from at least 5 images acquired from a tissue sample. Right panel: Violin plots show the quantitative assessment of *CSF2* mRNA (upper: MFI-red) and GM-CSF protein (lower: MFI-green) expression in HIV Negative donors (n = 12), and PWH (n = 10), (B) Positive correlations of *CSF2* mRNA and GM-CSF protein expression through combined FISH and immunofluorescence staining in the vascular endothelium obtained from negative controls (n = 12) and PWH (n = 10), (A: *p < 0.05).

(C) Measurement of GM-CSF levels in plasma samples obtained from HIV Neg. (n = 17) and PWH (n = 17) using ELISA., (*p < 0.05). All data are represented as mean ± SEM.

led to the reversal of LPS-induced ED, suggesting that downregulating glycolytic pathways with SGLT2 inhibitors may counterbalance ED in PWH.

RESULTS

In this study, we primarily focused on investigating the significance of persistent ED and endothelium-derived GM-CSF. We conducted experiments using primary human aortic ECs, vascular tissues, and plasma from both uninfected donors and PWH (See Supplemental for details).

Elevated expression of granulocyte macrophage-CSF mRNA (*CSF2*), GM-CSF in the vascular endothelium, and higher plasma levels of granulocyte macrophage-CSF in people with HIV

To determine if GM-CSF expression in the endothelium of major arteries was associated with atherosclerosis, we used immunofluorescence imaging to measure GM-CSF protein expression in commercially available coronary and internal carotid artery samples from people without HIV (see STAR Methods). We found that endothelial GM-CSF protein expression was higher in atherosclerotic tissues than in tissues without atherosclerosis (Figure S1).

We next asked if GM-CSF expression in atherosclerotic tissues was associated with HIV status. GM-CSF mRNA (*CSF2*) and protein levels were measured in the atherosclerotic endothelium of PWH and of controls without HIV who had undergone medically indicated vascular reconstruction surgeries (see study participant information in Table S1) using dual mRNA FISH and immunofluorescence staining (Figure 1A, left panel). Both *CSF2* mRNA and GM-CSF protein were significantly elevated (p < 0.05) in tissues from PWH when compared to tissues from controls without HIV (Figure 1A, right panel). This difference is particularly striking as the PWH were nearly 20 years younger than the HIV negative population (Table S1). Among all donors, irrespective of their HIV status, the intensity of tissue GM-CSF and *CSF2* staining was positively correlated (Figure 1C, R^2 = 0.86).

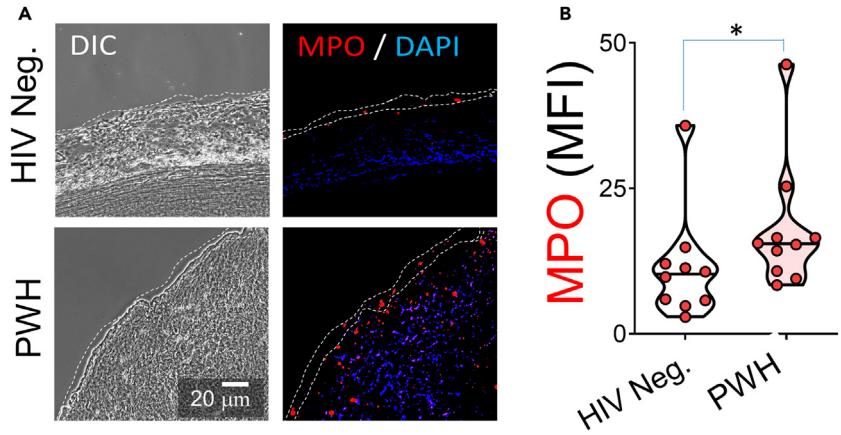

Figure 2. Myeloperoxidase levels in the endothelium and sub-endothelium of PWH

(A) Epi-fluorescent microscopy images depict myeloperoxidase (MPO, red) positive staining in the vascular endothelium and subendothelial tissues obtained from HIV Negative controls and PWH.

(B) Violin plots showing quantified MFI values of MPO expression in the vascular endothelium and subendothelial tissues of HIV Neg and PWH. Each circle represents the average fluorescence intensity data from at least 5 images acquired from a tissue sample. (HIV Neg., n = 12; and PWH, n = 10). (*$p < 0.05$). Data are represented as mean ± SEM.

Given the strong association of GM-CSF expression with HIV status in donors with peripheral vascular disease, we next tested if systemic levels of GM-CSF were generally elevated in PWH, using plasma from a second, separate population of PWH and age matched people without HIV (PWoH) controls (Table S2). Plasma GM-CSF levels were significantly higher in PWH than in PWoH (Figure 1D). LPS has been shown to induce expression of GM-CSF at both transcriptional and protein levels in human umbilical vein endothelial cells (HUVEC) and pulmonary alveolar epithelial cells.[19] In this study, we measured plasma LPS and GM-CSF levels in a subset of uninfected control donors and PWH. Our data is consistent with previous reports and indicates that LPS promotes endothelial GM-CSF expression in PWH, where we observed a positive correlation between plasma LPS and GM-CSF levels (Figure S2).

Increased myeloperoxidase expression in the aortic endothelium of people with HIV

Given the pro-inflammatory nature of GM-CSF as a myeloid growth factor, we explored the potential impact of local GM-CSF at the endothelial surface and sub-endothelium. We performed immunofluorescence staining for myeloperoxidase (MPO), a lineage specific molecule expressed by granulocytes, in order to elucidate the extent of potential neutrophil infiltration into the tissues of the PWH and controls with peripheral vascular disease (Figure 2). MPO protein expression (as estimated by the mean fluorescence intensity (MFI) of immunofluorescence staining) was significantly increased within both the vascular endothelium and subendothelial tissues in PWH when compared with the MFI values in the tissues from PWoH control group (Figure 2B).

Elevated expression of toll-like receptor-4 mRNA and higher surface toll-like receptor-4 protein levels in the vascular endothelium of people with HIV

Since TLR4 activation by microbial elements (such as LPS) stimulates a strong inflammatory response in microvascular ECs,[20] we next investigated TLR4 mRNA and protein expression in the aortic endothelium of PWH and PWoH controls, all of whom had undergone reconstructive vascular surgery for pre-existing atherosclerotic disease. We quantified the *TLR4* gene expression by RNA *in situ* hybridization. The number of *TLR4* mRNA was significantly higher in PWH than in controls without HIV (Figure 3A). Similarly, the relative expression of TLR4 protein (normalized to DAPI signal), was significantly higher in the vascular endothelium of PWH than in the vascular endothelium of the uninfected control group. Thus, vascular tissues of PWH with peripheral vascular disease have evidence of elevated GM-CSF, MPO, and TLR4 gene and protein expression when compared to tissues from controls with peripheral vascular disease but without HIV, even though the PWH are nearly 20 years younger.

Granulocyte macrophage-CSF expression is increased in aortic endothelial cells by other toll-like receptor ligands but most significantly by bacterial lipopolysaccharide, in a concentration dependent manner

We considered the possibility that bacterial products could contribute to the induction of GM-CSF release by human ECs.[3] We used immunofluorescence staining, microscopy, and image data analyses to detect and quantify GM-CSF and endothelial nitric oxide synthase (eNOS) protein expression in primary human aortic ECs (Figure 4A – left panel). Expression of GM-CSF and eNOS proteins was rapidly upregulated in the cytoplasmic compartments of EC within 4 h of LPS (100 ng/mL) exposure (Figure 4A – right panel). In addition to being detectable in the EC culture supernatant, GM-CSF was also detectable in EC-derived extracellular vesicles (EVs), including microvesicles and exosomes, following 24 h of LPS exposure (Figure 4B: see complete WB image in Figure S3C), suggesting that EV-associated GM-CSF could contribute

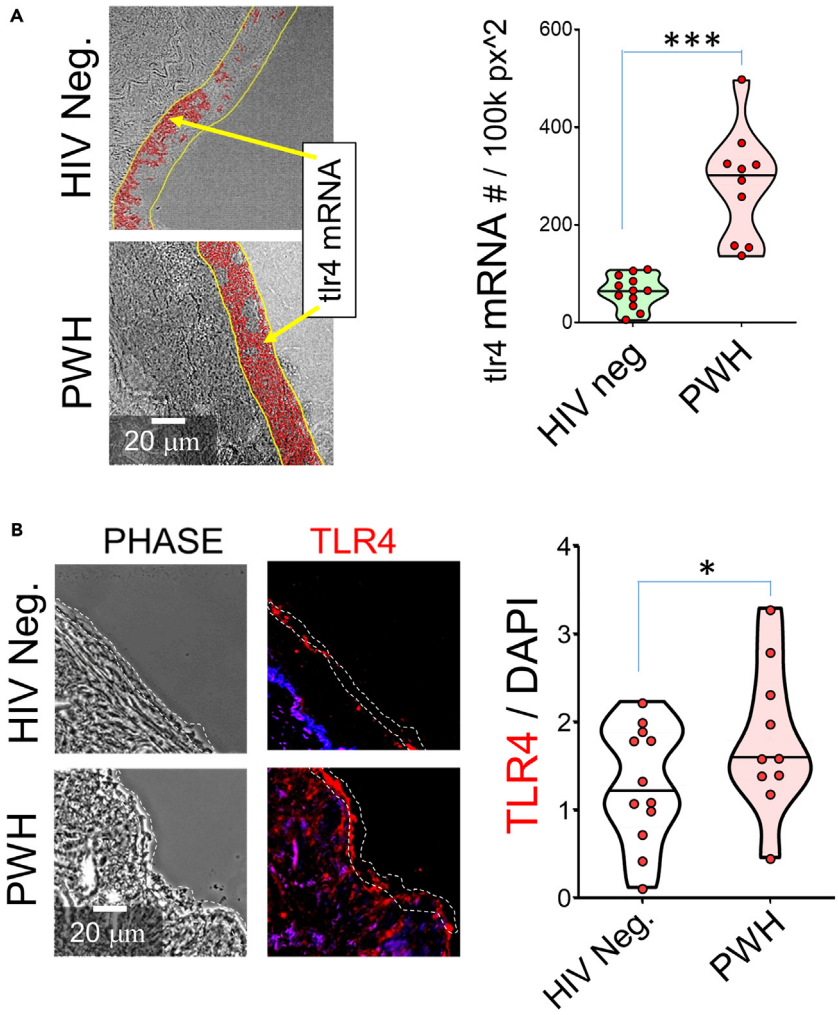

Figure 3. Quantitative analysis of toll-like receptor 4 (TLR4) gene and receptor expression in vascular endothelium of PWH

(A) *TLR4* mRNA copy number per 100k pixel^2 in the vascular endothelium and subendothelial tissues of uninfected controls (n = 12) and PWH (n = 10). (***$p < 0.0005$).

(B) TLR4 receptor expression in the vascular endothelium comparing uninfected controls and PWH (n = 22), (*$p < 0.05$). All data are represented as mean ± SEM.

to cellular communication between ECs and other cell types. Among the TLR ligands we tested, LPS uniquely induced both GM-CSF protein production and release into the medium (See STAR Methods for details) (Figures 4C, S3A, and S3B).

A unique cell cluster emerges from HAECs stimulated with lipopolysaccharide that is driven by pro-inflammatory gene expression signatures and downregulation of Krüppel-like factor 2

We next used single-cell RNA sequencing (scRNAseq) to study gene expression in EC cells exposed *ex vivo* for 24 h to LPS or to dapagliflozin (Dapa), an inhibitor of sodium-glucose cotransporter-2 (SGLT2). We performed uniform manifold approximation and projection (UMAP), a nonlinear dimensionality-reduction machine learning approach, to objectively determine the heterogeneity within the treated cell population and identified 5 unique clusters (labeled 0–4) across all treatments (Figure 5A). As part of a larger study, we also incubated ECs with estradiol to ascertain if this hormone might influence EC maturation. Data from the ECs treated with estradiol for 24 h or 7 days are included in the UMAP analysis and largely contributed to Clusters 2 and 3 (Figures 5A and 5B).

The transcriptional profile of cells within Cluster 4, which appeared to associate primarily with LPS-treated cells, was consistent with an inflammatory cell type, and when compared to cells in other clusters, included increased mRNA expression for genes involved in iron metabolism (FTH1), antiviral activity (ISG15, BST2), and chemoattraction of myeloid cells (IL-32, CXCL8, CXCL1) (Figure 5B). Expression of *KLF2* and *NOS3* (the gene for eNOS) trended to be diminished in cells from Cluster 4 when compared to cells from other clusters, while *ICAM1* and *VCAM1* trended to be increased, consistent with LPS-induced endothelial cell dysfunction. Moreover, when comparing the effects of LPS treatment versus medium control on cells that remained within Cluster 0, we found significantly reduced levels of *KLF2* and *NOS3* transcripts

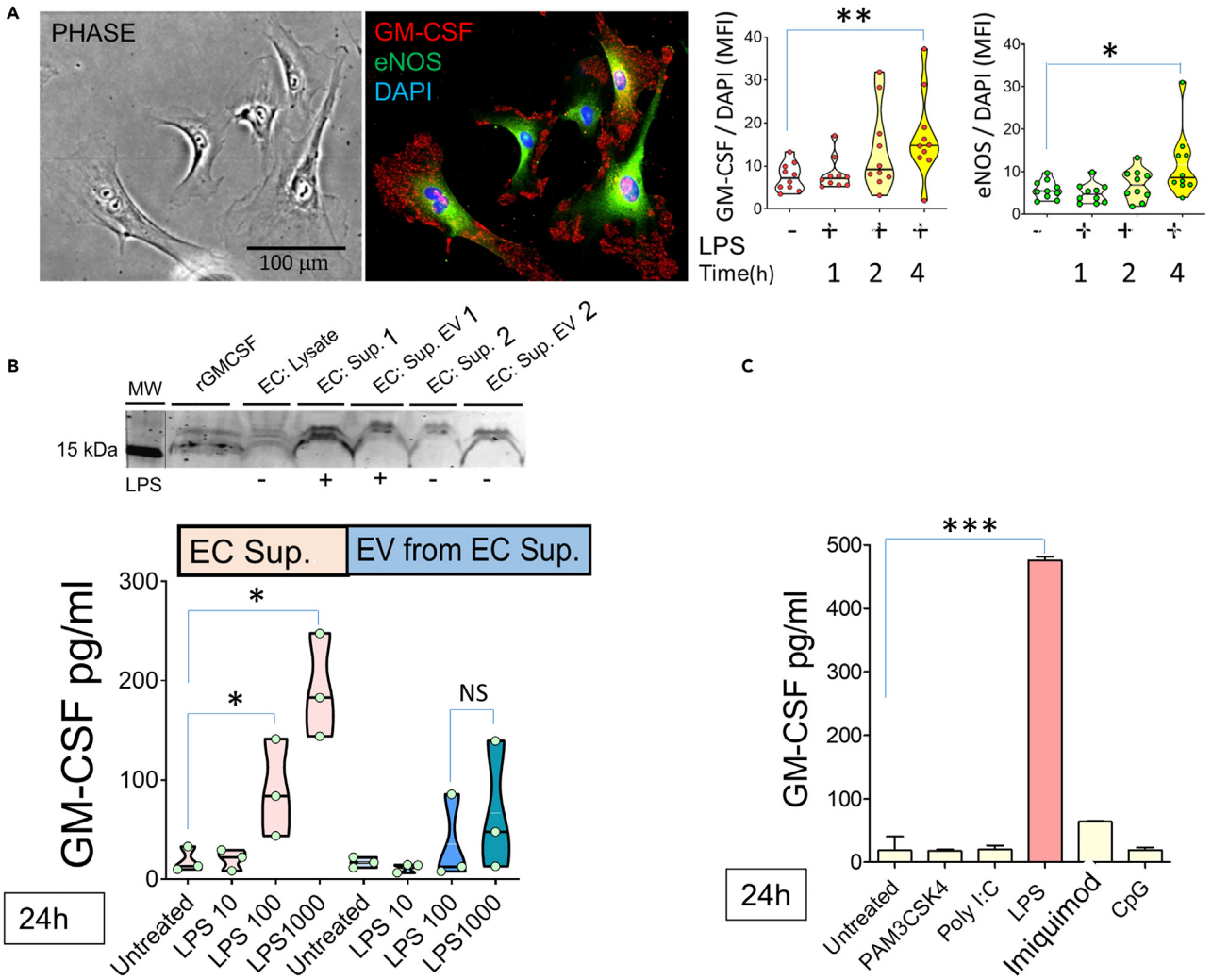

Figure 4. LPS-induced GM-CSF expression and release by human aortic endothelial cells

(A) Immunofluorescence microscopy image shows intracellular staining of GM-CSF (red), eNOS (green), and DAPI (blue) in primary human aortic endothelial cells (ECs). Time-dependent changes in intracellular GM-CSF and eNOS levels are quantified using the intracellular GM-CSF-to-DAPI MFI ratio and intracellular eNOS-to-DAPI MFI ratio. The image represents endothelial responses to LPS at indicated time points from one of the three identical experiments.

(B) (Top image) Detection of GM-CFS by Western Blot (see Figure S3C for the complete WB data) in EC supernatant and in purified, lysed EVs from cells stimulated overnight with LPS (100 ng/mL) or incubated without stimulation (supernatant 2). (Bottom image) ELISA data (n = 3) illustrating a dose-dependent increase in GM-CSF concentration in cell culture supernatants or in purified and lysed EVs, derived from culture supernatants following overnight incubation of ECs with or without exposure to LPS at varying concentrations. Data shown here (A, B) are from one of the 3 independent experiments, each circle represents average MFI values from one image with ~10 ECs, n = ~100 cells/experiment (*$p < 0.05$).

(C) GM-CSF detection in endothelial cell culture supernatants after overnight incubation with the indicated TLR agonists (n = 3, *$p < 0.05$). All data are represented as mean ± SEM.

in cells after LPS treatment (Data S1). Cells from Cluster 4 also trended to have increased *CSF2* and *CSF3* expression, but not *TLR4* expression (Figure 5D) (Data S2). Taken together, our findings are consistent with the interpretation that LPS can be a major inducer of EC activation and subsequent ED.

Attenuation of Granulocyte macrophage-CSF expression by pharmacological modulation of endothelial glucose uptake and toll-like receptor-4 blocking

Given the importance of cellular metabolism for inflammatory activity, we measured glucose uptake in primary human aortic ECs and found that stimulating these cells with LPS enhanced their uptake of fluorescent NBD glucose (Figure 6A). We then hypothesized that reducing glucose metabolism in ECs via inhibition of SGLT2 would limit ED and GM-CSF production in LPS-stimulated cells. SGLT2 is expressed on

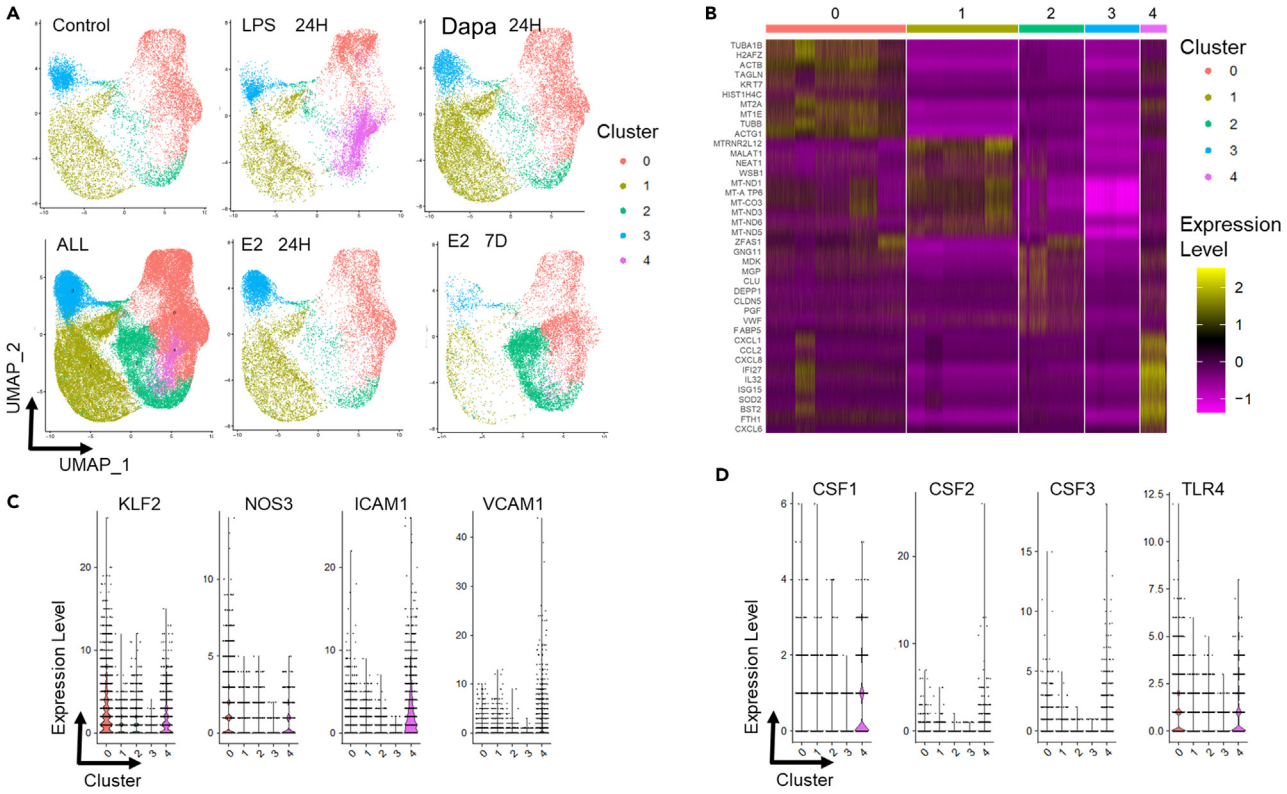

Figure 5. Single-cell RNA sequencing (RNAseq) reveals dynamic gene expression patterns in human aortic endothelial cells (ECs)

ECs were cultured in medium alone or medium supplemented with LPS (100 ng/mL) or Dapa (1μg/mL) for 24 h. An additional 7days incubation period was included for estradiol (10 ng/mL) only (D5-E2-D7).

(A). Unbiased clustering and UMAP representation of scRNAseq data analyzed with a resolution setting of 0.12, displaying distinct clusters of human aortic endothelial cells on a UMAP plot.

(B) HeatMap of treatment-dependent differentially expressed genes illustrates the differential expression of genes in ECs across various treatment conditions, highlighting treatment-dependent clusters.

(C and D) Violin plots display the expression profiles of selected genes (KLF2, eNOS, ICAM-1, VCAM-1, CSF-1, CSF2, and CSF3) within clusters from LPS treated cells. Expression levels are represented as probability distributions across clusters on the y axis.

ECs (Figure S4A),[21,22] and others have shown that SGLT2 can be upregulated in these cells by exposure to high glucose concentrations.[23,24] While the treatment of ECs with dapagliflozin (Dapa), an inhibitor with strong binding affinity to SGLT2 (Figure S4B), did not substantially alter the EC transcriptome (Figure 5A), Dapa treatment did significantly reduce the LPS-mediated enhancement of NBD glucose uptake by ECs (Figure 6A). This effect was comparable to direct TLR4 receptor inhibition (Figure 6A). In addition, Dapa partially protected ECs from LPS-mediated down-modulation of KLF2 expression (Figure 6B). Furthermore, Dapa lowered LPS-induced GM-CSF release by ECs (Figure 6C). Results from clinical trials have demonstrated that SGLT2 inhibitors improve cardiovascular disease (CVD) outcomes in individuals with type 2 diabetes.[25,26] We found that PWH with type 2 diabetes receiving Dapa had lower plasma GM-CSF levels than did PWH without diabetes or Dapa treatment (Figure 6D).

DISCUSSION

Inflammation and inflammation-associated endothelial dysfunction (ED) underpin the development of arterial, venous, and microvascular diseases in people with and without HIV. Factors secreted by macrophages activate human vascular ECs and trigger the expression of G-CSF, GM-CSF, and IL-6 where the heightened levels of plasma IL-6 have been linked to increased risk of CVD in PWH.[27] Activation of myeloid cells in HIV is thought to stem, at least in part, from increased translocation of microbial products across a damaged gut barrier and could theoretically play a role in crosstalk between myeloid cells and endothelium.[27–31] Our data suggest that circulating microbial products may also directly induce the activation of ECs, potentially contributing to the increased ED in PWH.[14]

Here, we report that there is an increase in both gene and protein expression of GM-CSF within the vascular endothelium, as well as significantly elevated plasma GM-CSF levels, in PWH. In comparing the arterial endothelium of people with and without HIV, all of whom had peripheral vascular disease requiring vascular reconstructive surgery, we also uncovered evidence of neutrophil activation as indicated by

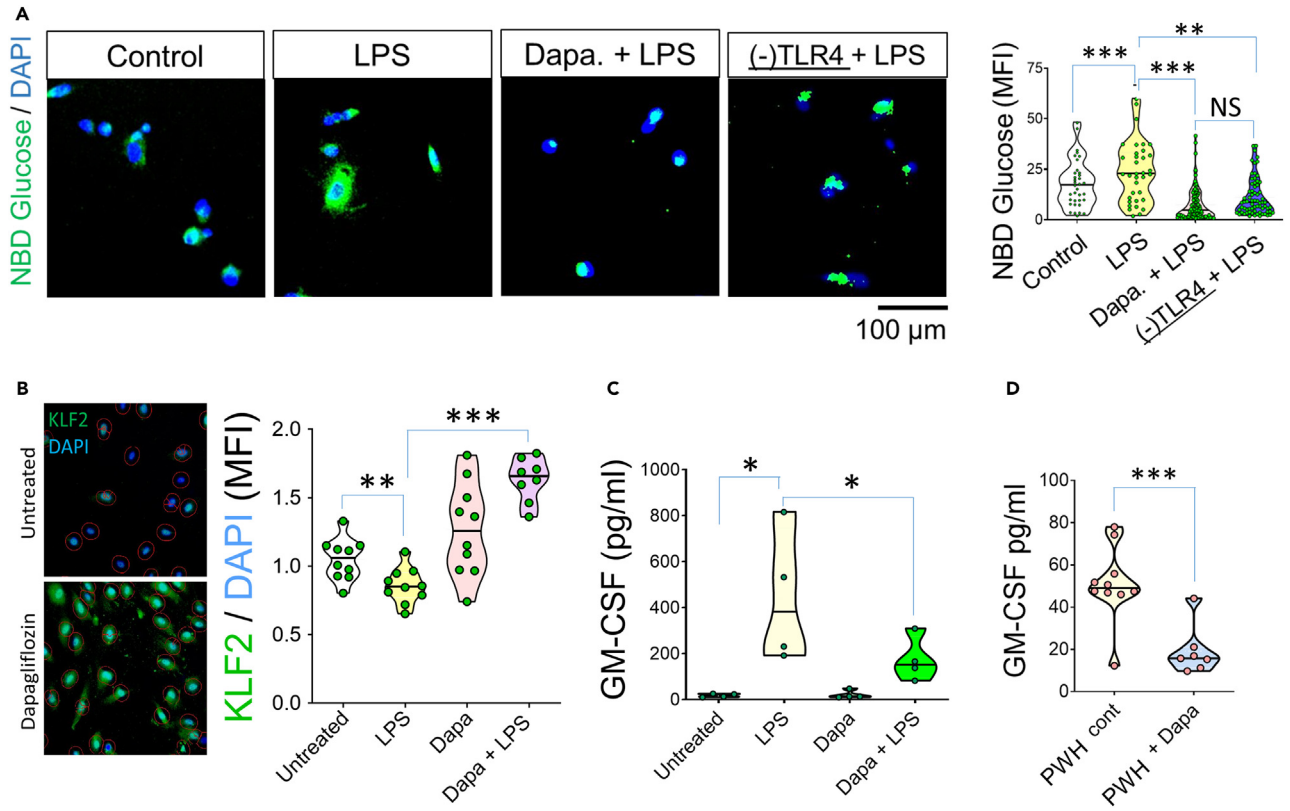

Figure 6. Modulation of LPS-induced GM-CSF expression by human aortic endothelial cells (EC) through pharmacological interventions

Endothelial cells were cultured in medium alone or medium supplemented with LPS (100 ng/mL), LPS + Dapa (1µg/mL) or LPS + TLR-4 Inhibitor (TLR4-C34) (10µg/mL).

(A) Representative microscopy and fluorescent images of NBD glucose uptake under the indicated conditions (left) and violin plots show the quantification of NBD glucose uptake (MFI, right) in EC receiving indicated treatments (data from one of the 3 independent experiments, each circle represents MFI value from one EC, n = ∼100 cells/experiment, ***$p < 0.0005$).

(B) Immunofluorescence microscopy images (left) and violin plots showing quantified image data (MFI/DAPI ratio, right) illustrating KLF2 protein expression in indicated treatment groups (data from 100 ECs per condition; each circle represents average MFI values from one image with 5–10 ECs).

(C) ELISA data illustrate GM-CSF protein concentrations in supernatants of endothelial cell cultures after 24 h of incubation under specified conditions (n = 3; *$p < 0.05$).

(D) Violin plots show ELISA data of GM-CSF levels in plasma samples from PWH, with (n = 7) and without (n = 10) receiving Dapa treatment (***$p < 0.0005$). All data are represented as mean ± SEM.

elevated expression of myeloperoxidase (MPO). MPO is a highly basic protein produced by neutrophils that binds to the surface of negatively charged cells, potentially enabling antimicrobial responses. Although the classical MPO-halide-H_2O_2 system is an effective antimicrobial mechanism, MPO can also damage the adjacent cells in host tissues and contribute to human disease.[32,33] Consequently, the potent oxidation system of leukocyte MPO can have adverse effects at the blood-endothelial interface and in the subendothelial space.[34] Our findings of elevated GM-CSF and MPO levels in the atherosclerotic endothelium suggest a possible role for these pathways in the pathogenesis of atherosclerosis in PWH.[35]

We also report that both TLR4 gene and protein expression are significantly elevated in the vascular endothelium of PWH compared to tissues from control individuals without HIV. This observation raises the possibility that sensitivity to TLR4 agonists may be enhanced in the vascular endothelium of PWH. Combined with evidence of heightened LPS concentrations in the plasma of PWH, these findings suggest that the LPS/TLR4 pathway is potentially a direct mediator of ED in HIV disease. Although we show here that LPS can directly activate ECs *in vitro*, the possibility that other TLR4 agonists might contribute to endothelial pathology in PWH may be worth further exploration. For instance, free hemoglobin and heme, which are both danger-associated molecular patterns (DAMPs) that engage TLR4,[36] have been found elevated in some PWH and could plausibly contribute to inducing GM-CSF expression.[37–39]

Recently, it was reported that PWH exhibit a persistent pro-inflammatory profile with elevated levels inflammatory mediators including GM-CSF, even with early-initiated antiretroviral treatment.[40] The cellular origins of GM-CSF measured in plasma have not been determined. Conceptually, GM-CSF associated with EVs could provide clues as to the origins of this cytokine in circulation and our data indicate that EV-associated GM-CSF can be released from ECs. Given the capacity of EVs to mediate intercellular communication, and the capacity of EVs to

deliver cytokines that trigger cellular responses,[41] our findings highlight a possible role for GM-CSF-carrying EVs from the endothelium as a conduit for inflammation in PWH.[42] Studies that define cytokine content in specific EV subsets in plasma may be useful in exploring this possibility.

Our single-cell RNA sequencing (scRNAseq) data provide insights into the complexities of EC gene expression resulting from LPS exposure. In particular, proportional changes were observed in cellular subsets defined by cluster analysis in cells incubated with LPS with one novel cluster of cells emerging from the total population as a consequence of LPS stimulation (Cluster 4), with a trend toward increased *CSF2* expression in this cluster. Incubation of ECs with Dapa, in contrast, did not appear to markedly alter EC clusters. We found that the incubation of cells with LPS downregulates *KLF2* and *NOS3*, which are involved in the maintenance of endothelial function and increased the expression of endothelial adhesion molecules *ICAM1* and *VCAM1*, even in cells that clustered with the major population of control, untreated cells (Cluster 0). Further studies may be helpful in defining the clusters of ECs that appear to respond differently to LPS stimulation, in order to ascertain if such populations are discernable *in vivo*.

Ongoing inflammation as identified by increased fluoro-2-deoxy-D-glucose uptake within arterial walls is indicative of predilection to increased CVD in PWH.[43] Here, we demonstrated that SGLT2 inhibition reduced LPS-driven endothelial glucose uptake, ED, and GM-CSF expression. Plasma samples obtained from PWH receiving Dapa for type 2 diabetes treatment had lower levels of GM-CSF than did samples from PWH without diabetes (or Dapa), suggesting a possible role of SGLT2 inhibitors in mitigating ED in PWH.

In multiple recent clinical trials, SGLT2 inhibitors have been proven highly effective in lowering the occurrence and progression of CVD and related mortality, where the underlying mechanisms of these beneficial effects were not clearly elucidated.[26,44–46] Previous studies have indicated that ED in diabetics is linked to endothelial responses triggered by glucose and other stressors, including oxidative free radicals and thrombin. These factors contribute to an upregulation of SGLT2 mRNA and protein expression,[47,48] while ensuring a balanced nutrient transport and glucose distribution across the endothelium is essential for maintaining endothelial health. In another report, glycemic regulation by SGLT2 inhibitors such as Dapa reversed ED improving NO bioavailability and reducing ROS and protein kinase C signaling in human coronary artery endothelium.[49] Here, our *in vitro* observations also indicate that SGLT2 inhibition could protect the endothelium from ED induced by LPS-mediated downregulation of KLF2 while downmodulating GM-CSF release. This observation is consistent with the earlier reports of an endothelial protective effect of SGLT2 inhibitors.

In summary, our data point to an intricate interplay involving TLR4 engagement, GM-CSF release, and ED, all of which might contribute to the increased risk of CVD in PWH. We propose that elevated expression of TLR4, plasma levels of LPS, and increased GM-CSF as potential contributors to the persistent pro-inflammatory state in PWH, particularly in atherosclerotic arterial tissues. Our data suggests that utilizing SGLT2 inhibitors could reduce glucose uptake and GM-CSF expression in the endothelium, holding promise for therapeutic outcomes by mitigating the pathological consequences of ED in PWH.

Limitations of the study

We acknowledge limitations. First, the number of vascular tissue donors was relatively small, and they were almost exclusively black South Africans from whom we did not have age and gender matched plasma samples (Table S1). Indeed, all the plasma samples we used in this study were obtained from an independent population of North American PWH and PWoH control donors, comprising both White and Black participants (Table S2). Second, we did not investigate, if the plasma GM-CSF levels are lower in diabetics without HIV who also received SGLT2 inhibitors, - an analysis we intend to include in our future studies. Third, we employed a specific relatively higher concentration of LPS (100 ng/mL) and dose response in our *in vitro* experiments, which yielded results (Figure 4B) comparable to previous reports.[14] Finally, our pilot single-cell RNA sequencing study of the ECs was originally designed to include three biological replicates ($n = 3$) per condition. However, due to technical constraints, here we presented data from a single set of experiments for each experimental condition. To minimize this limitation, we incorporated the cumulative scRNAseq data from a large number of ECs (10,000 cells) within each experimental group. We also faced the limitations of not being able to use more than three fluorochromes for our immunofluorescence microscopy, but we chose to maintain consistent tissue staining and microscopy protocols throughout the study. Although automated multiplex immunofluorescence microscopy and data analysis would have been preferable, our approach ensured uniformity in data acquisition.

RESOURCE AVAILABILITY

Lead contact

Further information and requests for resources and reagents should be directed to and will be fulfilled by the lead contact, Soumya Panigrahi (sxp579@case.edu).

Materials availability

This study did generate new unique resources. We constructed a vascular tissue microarray FFPE block from de-identified HIV positive (PWH) and uninfected control subjects. We also used commercially available tissue microarray slides (AR301), which are available for purchase directly from US BioMax (www.biomax.us).

The human plasma samples were obtained from Rustbelt Sample Repository Core services. CFAR Core D: Clinical Sciences (Contact PI/Project Leader JACOBSON, JEFFREY M.) (https://reporter.nih.gov/search/BOh9K9dktEqRjs89F56gVg/project-details/10615816) at Case Western Reserve University, Cleveland, Ohio, USA.

Data and code availability

- Data availability: All data including the Original western blot images have been deposited at Mendeley and are also publicly available as of the date of publication. Accession numbers and the DOI are listed in the key resources table. Microscopy image data reported in this article will be shared by the lead contact upon request. Any additional information required to reanalyze the data reported in this article is available from the lead contact upon request.
- Code availability: Not applicable.

ACKNOWLEDGMENTS

We sincerely thank Mary Midea, Daniela Moisi, Brian M. Clagett, Dominic Dorazio, Douglas A. Bazdar, and Tamal Goswami for administrative and technical assistance. SP sincerely thanks his Rustbelt CFAR mentors: Alan D. Levine, Mark J. Cameron, Cheryl M. Cameron, Nicolas P. Sluis-Cremer, and Charles R. Rinaldo.

Funding: This work was primarily supported by –

- Career development award to SP from RustBelt CFAR (NIAID: AI036219).

- NIH R21 TO MLF AI162150.

- CFAR GRANTS: NIH/NIAID: 5P30AI036219-27; and NIH/NIAID: AI36219 TO Mark Cameron.

- Grants from Fasenmyer Foundation, and the Case Western Reserve University Center for AIDS Research.

- This project was supported in part by the Clinical and Translational Science Collaborative of Northern Ohio, which is funded by the National Institutes of Health, National Center for Advancing Translational Sciences, Clinical and Translational Science Award grant, UM1TR004528. The content is solely the responsibility of the authors and does not necessarily represent the official views of the NIH.

AUTHOR CONTRIBUTIONS

Conceptualization: SP, MML, and SFS; methodology: SP, EM, SL, and AC; investigation: SP, NTF, JMJ, SMC, and SFS; visualization: SP and AC. Funding acquisition: SP, MML, MLF, and SFS; project administration: SP; supervision: SP, MML, MLF, and SFS; writing, – original draft: SP; writing – review and editing: SP, EM, JMJ, MML, MLF, and SFS.

DECLARATION OF INTERESTS

The authors declare no competing interests.

STAR★METHODS

Detailed methods are provided in the online version of this paper and include the following:

SUPPLEMENTAL INFORMATION

Supplemental information can be found online at https://doi.org/10.1016/j.isci.2024.110909.

Received: December 21, 2023
Revised: June 29, 2024
Accepted: September 5, 2024
Published: September 11, 2024

REFERENCES

1. Quesenberry, P.J., and Gimbrone, M.A., Jr. (1980). Vascular endothelium as a regulator of granulopoiesis: production of colony-stimulating activity by cultured human endothelial cells. Blood *56*, 1060–1067.
2. Ascensao, J.L., Vercellotti, G.M., Jacob, H.S., and Zanjani, E.D. (1984). Role of endothelial cells in human hematopoiesis: modulation of mixed colony growth in vitro. Blood *63*, 553–558.
3. Zsebo, K.M., Yuschenkoff, V.N., Schiffer, S., Chang, D., McCall, E., Dinarello, C.A., Brown, M.A., Altrock, B., and Bagby, G.C., Jr. (1988). Vascular endothelial cells and granulopoiesis: interleukin-1 stimulates release of G-CSF and GM-CSF. Blood *71*, 99–103.
4. Bagby, G.C., Jr., Shaw, G., and Segal, G.M. (1989). Human vascular endothelial cells, granulopoiesis, and the inflammatory response. J. Invest. Dermatol. *93*, 48S–52S. https://doi.org/10.1111/1523-1747.ep12580910.
5. Becher, B., Tugues, S., and Greter, M. (2016). GM-CSF: From Growth Factor to Central Mediator of Tissue Inflammation. Immunity *45*, 963–973. https://doi.org/10.1016/j.immuni.2016.10.026.
6. Lee, K.M.C., Achuthan, A.A., and Hamilton, J.A. (2020). GM-CSF: A Promising Target in Inflammation and Autoimmunity.

ImmunoTargets Ther. *9*, 225–240. https://doi.org/10.2147/ITT.S262566.
7. Konradt, C., and Hunter, C.A. (2018). Pathogen interactions with endothelial cells and the induction of innate and adaptive immunity. Eur. J. Immunol. *48*, 1607–1620. https://doi.org/10.1002/eji.201646789.
8. Lerman, A., and Burnett, J.C., Jr. (1992). Intact and altered endothelium in regulation of vasomotion. Circulation *86*. III12–19.
9. Mayne, E.S., and Louw, S. (2019). Good Fences Make Good Neighbors: Human Immunodeficiency Virus and Vascular Disease. Open Forum Infect. Dis. *6*, ofz303. https://doi.org/10.1093/ofid/ofz303.
10. SenBanerjee, S., Lin, Z., Atkins, G.B., Greif, D.M., Rao, R.M., Kumar, A., Feinberg, M.W., Chen, Z., Simon, D.I., Luscinskas, F.W., et al. (2004). KLF2 Is a novel transcriptional regulator of endothelial proinflammatory activation. J. Exp. Med. *199*, 1305–1315. https://doi.org/10.1084/jem.20031132.
11. Landmesser, U., Hornig, B., and Drexler, H. (2004). Endothelial function: a critical determinant in atherosclerosis? Circulation *109*. II27–33. https://doi.org/10.1161/01.CIR.0000129501.88485.1f.
12. Hadi, H.A.R., Carr, C.S., and Al Suwaidi, J. (2005). Endothelial dysfunction: cardiovascular risk factors, therapy, and outcome. Vasc. Health Risk Manag. *1*, 183–198.
13. Zevin, A.S., McKinnon, L., Burgener, A., and Klatt, N.R. (2016). Microbial translocation and microbiome dysbiosis in HIV-associated immune activation. Curr. Opin. HIV AIDS *11*, 182–190. https://doi.org/10.1097/COH.0000000000000234.
14. Panigrahi, S., Freeman, M.L., Funderburg, N.T., Mudd, J.C., Younes, S.A., Sieg, S.F., Zidar, D.A., Paiardini, M., Villinger, F., Calabrese, L.H., et al. (2016). SIV/SHIV Infection Triggers Vascular Inflammation, Diminished Expression of Kruppel-like Factor 2 and Endothelial Dysfunction. J. Infect. Dis. *213*, 1419–1427. https://doi.org/10.1093/infdis/jiv749.
15. Akira, S., Takeda, K., and Kaisho, T. (2001). Toll-like receptors: critical proteins linking innate and acquired immunity. Nat. Immunol. *2*, 675–680. https://doi.org/10.1038/90609.
16. Klatt, N.R., Chomont, N., Douek, D.C., and Deeks, S.G. (2013). Immune activation and HIV persistence: implications for curative approaches to HIV infection. Immunol. Rev. *254*, 326–342. https://doi.org/10.1111/imr.12065.
17. Luo, Z., Health, S.L., Li, M., Yang, H., Wu, Y., Collins, M., Deeks, S.G., Martin, J.N., Scott, A., and Jiang, W. (2022). Variation in blood microbial lipopolysaccharide (LPS) contributes to immune reconstitution in response to suppressive antiretroviral therapy in HIV. EBioMedicine *80*, 104037. https://doi.org/10.1016/j.ebiom.2022.104037.
18. Oblak, A., and Jerala, R. (2015). The molecular mechanism of species-specific recognition of lipopolysaccharides by the MD-2/TLR4 receptor complex. Mol. Immunol. *63*, 134–142. https://doi.org/10.1016/j.molimm.2014.06.034.
19. Burg, J., Krump-Konvalinkova, V., Bittinger, F., and Kirkpatrick, C.J. (2002). GM-CSF expression by human lung microvascular endothelial cells: in vitro and in vivo findings. Am. J. Physiol. Lung Cell Mol. Physiol. *283*, L460–L467. https://doi.org/10.1152/ajplung.00249.2001.
20. Bryant, C.E., Spring, D.R., Gangloff, M., and Gay, N.J. (2010). The molecular basis of the host response to lipopolysaccharide. Nat. Rev. Microbiol. *8*, 8–14. https://doi.org/10.1038/nrmicro2266.
21. Li, C.Y., Wang, L.X., Dong, S.S., Hong, Y., Zhou, X.H., Zheng, W.W., and Zheng, C. (2018). Phlorizin Exerts Direct Protective Effects on Palmitic Acid (PA)-Induced Endothelial Dysfunction by Activating the PI3K/AKT/eNOS Signaling Pathway and Increasing the Levels of Nitric Oxide (NO). Med. Sci. Monit. Basic Res. *24*, 1–9. https://doi.org/10.12659/msmbr.907775.
22. Wicik, Z., Nowak, A., Jarosz-Popek, J., Wolska, M., Eyileten, C., Siller-Matula, J.M., von Lewinski, D., Sourij, H., Filipiak, K.J., and Postuła, M. (2022). Characterization of the SGLT2 Interaction Network and Its Regulation by SGLT2 Inhibitors: A Bioinformatic Analysis. Front. Pharmacol. *13*, 901340. https://doi.org/10.3389/fphar.2022.901340.
23. Clyne, A.M. (2021). Endothelial response to glucose: dysfunction, metabolism, and transport. Biochem. Soc. Trans. *49*, 313–325. https://doi.org/10.1042/BST20200611.
24. D'Onofrio, N., Sardu, C., Trotta, M.C., Scisciola, L., Turriziani, F., Ferraraccio, F., Panarese, I., Petrella, L., Fanelli, M., Modugno, P., et al. (2021). Sodium-glucose co-transporter2 expression and inflammatory activity in diabetic atherosclerotic plaques: Effects of sodium-glucose co-transporter2 inhibitor treatment. Mol. Metab. *54*, 101337. https://doi.org/10.1016/j.molmet.2021.101337.
25. Furtado, R.H.M., Bonaca, M.P., Raz, I., Zelniker, T.A., Mosenzon, O., Cahn, A., Kuder, J., Murphy, S.A., Bhatt, D.L., Leiter, L.A., et al. (2019). Dapagliflozin and Cardiovascular Outcomes in Patients With Type 2 Diabetes Mellitus and Previous Myocardial Infarction. Circulation *139*, 2516–2527. https://doi.org/10.1161/CIRCULATIONAHA.119.039996.
26. Wiviott, S.D., Raz, I., Bonaca, M.P., Mosenzon, O., Kato, E.T., Cahn, A., Silverman, M.G., Zelniker, T.A., Kuder, J.F., Murphy, S.A., et al. (2019). Dapagliflozin and Cardiovascular Outcomes in Type 2 Diabetes. N. Engl. J. Med. *380*, 347–357. https://doi.org/10.1056/NEJMoa1812389.
27. Shive, C.L., Biancotto, A., Funderburg, N.T., Pilch-Cooper, H.A., Valdez, H., Margolis, L., Sieg, S.F., McComsey, G.A., Rodriguez, B., and Lederman, M.M. (2012). HIV-1 is not a major driver of increased plasma IL-6 levels in chronic HIV-1 disease. J. Acquir. Immune Defic. Syndr. *61*, 145–152. https://doi.org/10.1097/QAI.0b013e31825ddbbf.
28. Yaseen, M.M., Abuharfeil, N.M., and Darmani, H. (2023). The role of IL-1beta during human immunodeficiency virus type 1 infection. Rev. Med. Virol. *33*, e2400. https://doi.org/10.1002/rmv.2400.
29. Doitsh, G., Galloway, N.L.K., Geng, X., Yang, Z., Monroe, K.M., Zepeda, O., Hunt, P.W., Hatano, H., Sowinski, S., Muñoz-Arias, I., and Greene, W.C. (2014). Cell death by pyroptosis drives CD4 T-cell depletion in HIV-1 infection. Nature *505*, 509–514. https://doi.org/10.1038/nature12940.
30. Pontillo, A., Silva, L.T., Oshiro, T.M., Finazzo, C., Crovella, S., and Duarte, A.J.S. (2012). HIV-1 induces NALP3-inflammasome expression and interleukin-1beta secretion in dendritic cells from healthy individuals but not from HIV-positive patients. AIDS *26*, 11–18. https://doi.org/10.1097/QAD.0b013e32834d697f.
31. Bowman, E.R., Cameron, C.M., Richardson, B., Kulkarni, M., Gabriel, J., Cichon, M.J., Riedl, K.M., Mustafa, Y., Cartwright, M., Snyder, B., et al. (2020). Macrophage maturation from blood monocytes is altered in people with HIV, and is linked to serum lipid profiles and activation indices: A model for studying atherogenic mechanisms. PLoS Pathog. *16*, e1008869. https://doi.org/10.1371/journal.ppat.1008869.
32. Hartman, C.L., and Ford, D.A. (2018). MPO (Myeloperoxidase) Caused Endothelial Dysfunction. Arterioscler. Thromb. Vasc. Biol. *38*, 1676–1677. https://doi.org/10.1161/ATVBAHA.118.311427.
33. Klebanoff, S.J. (1968). Myeloperoxidase-halide-hydrogen peroxide antibacterial system. J. Bacteriol. *95*, 2131–2138. https://doi.org/10.1128/jb.95.6.2131-2138.1968.
34. Manchanda, K., Kolarova, H., Kerkenpaß, C., Mollenhauer, M., Vitecek, J., Rudolph, V., Kubala, L., Baldus, S., Adam, M., and Klinke, A. (2018). MPO (Myeloperoxidase) Reduces Endothelial Glycocalyx Thickness Dependent on Its Cationic Charge. Arterioscler. Thromb. Vasc. Biol. *38*, 1859–1867. https://doi.org/10.1161/ATVBAHA.118.311143.
35. Zeng, L., Mathew, A.V., Byun, J., Atkins, K.B., Brosius, F.C., 3rd, and Pennathur, S. (2018). Myeloperoxidase-derived oxidants damage artery wall proteins in an animal model of chronic kidney disease-accelerated atherosclerosis. J. Biol. Chem. *293*, 7238–7249. https://doi.org/10.1074/jbc.RA117.000559.
36. Figueiredo, R.T., Fernandez, P.L., Mourao-Sa, D.S., Porto, B.N., Dutra, F.F., Alves, L.S., Oliveira, M.F., Oliveira, P.L., Graça-Souza, A.V., and Bozza, M.T. (2007). Characterization of heme as activator of Toll-like receptor 4. J. Biol. Chem. *282*, 20221–20229. https://doi.org/10.1074/jbc.M610737200.
37. Schaer, D.J., Vinchi, F., Ingoglia, G., Tolosano, E., and Buehler, P.W. (2014). Haptoglobin, hemopexin, and related defense pathways-basic science, clinical perspectives, and drug development. Front. Physiol. *5*, 415. https://doi.org/10.3389/fphys.2014.00415.
38. Chatterjee, T., Arora, I., Underwood, L., Gryshyna, A., Lewis, T.L., Masjoan Juncos, J.X., Goodin, B.R., Heath, S., and Aggarwal, S. (2023). High Heme and Low Heme Oxygenase-1 Are Associated with Mast Cell Activation/Degranulation in HIV-Induced Chronic Widespread Pain. Antioxidants *12*, 1213. https://doi.org/10.3390/antiox12061213.
39. Kebede, S.S., Yalew, A., Yesuf, T., Melku, M., Bambo, G.M., and Woldu, B. (2022). The magnitude and associated factors of immune hemolytic anemia among human immuno deficiency virus infected adults attending University of Gondar comprehensive specialized hospital north west Ethiopia 2021 GC, cross sectional study design. PLoS One *17*, e0274464. https://doi.org/10.1371/journal.pone.0274464.
40. De Clercq, J., De Scheerder, M.A., Mortier, V., Verhofstede, C., Vandecasteele, S.J., Allard, S.D., Necsoi, C., De Wit, S., Gerlo, S., and Vandekerckhove, L. (2023). Longitudinal patterns of inflammatory mediators after acute HIV infection correlate to intact and total reservoir. Front. Immunol. *14*, 1337316. https://doi.org/10.3389/fimmu.2023.1337316.
41. Komissarov, A., Potashnikova, D., Freeman, M.L., Gontarenko, V., Maytesyan, D.,

Lederman, M.M., Vasilieva, E., and Margolis, L. (2021). Driving T cells to human atherosclerotic plaques: CCL3/CCR5 and CX3CL1/CX3CR1 migration axes. Eur. J. Immunol. *51*, 1857–1859. https://doi.org/10.1002/eji.202049004.

42. Poveda, E., Tabernilla, A., Fitzgerald, W., Salgado-Barreira, Á., Grandal, M., Pérez, A., Mariño, A., Álvarez, H., Valcarce, N., González-García, J., et al. (2022). Massive Release of CD9+ Microvesicles in Human Immunodeficiency Virus Infection, Regardless of Virologic Control. J. Infect. Dis. *225*, 1040–1049. https://doi.org/10.1093/infdis/jiaa375.
43. Subramanian, S., Tawakol, A., Burdo, T.H., Abbara, S., Wei, J., Vijayakumar, J., Corsini, E., Abdelbaky, A., Zanni, M.V., Hoffmann, U., et al. (2012). Arterial inflammation in patients with HIV. JAMA *308*, 379–386. https://doi.org/10.1001/jama.2012.6698.
44. Uthman, L., Homayr, A., Juni, R.P., Spin, E.L., Kerindongo, R., Boomsma, M., Hollmann, M.W., Preckel, B., Koolwijk, P., van Hinsbergh, V.W.M., et al. (2019). Empagliflozin and Dapagliflozin Reduce ROS Generation and Restore NO Bioavailability in Tumor Necrosis Factor alpha-Stimulated Human Coronary Arterial Endothelial Cells. Cell. Physiol. Biochem. *53*, 865–886. https://doi.org/10.33594/000000178.
45. El-Daly, M., Pulakazhi Venu, V.K., Saifeddine, M., Mihara, K., Kang, S., Fedak, P.W.M., Alston, L.A., Hirota, S.A., Ding, H., Triggle, C.R., and Hollenberg, M.D. (2018). Hyperglycaemic impairment of PAR2-mediated vasodilation: Prevention by inhibition of aortic endothelial sodium-glucose-co-Transporter-2 and minimizing oxidative stress. Vascul. Pharmacol. *109*, 56–71. https://doi.org/10.1016/j.vph.2018.06.006.
46. Neal, B., Perkovic, V., and Matthews, D.R. (2017). Canagliflozin and Cardiovascular and Renal Events in Type 2 Diabetes. N. Engl. J. Med. *377*, 2099. https://doi.org/10.1056/NEJMc1712572.
47. Dhar-Mascareno, M., Chen, J., Zhang, R.H., Cárcamo, J.M., and Golde, D.W. (2003). Granulocyte-macrophage colony-stimulating factor signals for increased glucose transport via phosphatidylinositol 3-kinase- and hydrogen peroxide-dependent mechanisms. J. Biol. Chem. *278*, 11107–11114. https://doi.org/10.1074/jbc.M212541200.
48. McCoy, K.D., Ahmed, N., Tan, A.S., and Berridge, M.V. (1997). The hemopoietic growth factor, interleukin-3, promotes glucose transport by increasing the specific activity and maintaining the affinity for glucose of plasma membrane glucose transporters. J. Biol. Chem. *272*, 17276–17282. https://doi.org/10.1074/jbc.272.28.17276.
49. Alshnbari, A.S., Millar, S.A., O'Sullivan, S.E., and Idris, I. (2020). Effect of Sodium-Glucose Cotransporter-2 Inhibitors on Endothelial Function: A Systematic Review of Preclinical Studies. Diabetes Ther. *11*, 1947–1963. https://doi.org/10.1007/s13300-020-00885-z.
50. Schindelin, J., Arganda-Carreras, I., Frise, E., Kaynig, V., Longair, M., Pietzsch, T., Preibisch, S., Rueden, C., Saalfeld, S., Schmid, B., et al. (2012). Fiji: an open-source platform for biological-image analysis. Nat. Methods *9*, 676–682. https://doi.org/10.1038/nmeth.2019.
51. Bankhead, P., Loughrey, M.B., Fernández, J.A., Dombrowski, Y., McArt, D.G., Dunne, P.D., McQuaid, S., Gray, R.T., Murray, L.J., Coleman, H.G., et al. (2017). QuPath: Open source software for digital pathology image analysis. Sci. Rep. *7*, 16878. https://doi.org/10.1038/s41598-017-17204-5.
52. Wagstaff, K.M., Glover, D.J., Tremethick, D.J., and Jans, D.A. (2007). Histone-mediated transduction as an efficient means for gene delivery. Mol. Ther. *15*, 721–731. https://doi.org/10.1038/sj.mt.6300093.

STAR★METHODS

KEY RESOURCES TABLE

REAGENT or RESOURCE	SOURCE	IDENTIFIER
Antibodies		
Mouse monoclonal anti-human GM-CSF	R&D Systems	MAB215-100, Clone#3209
Rabbit polyclonal anti-eNOS	AbCam	phospho-S1177, ab75639
Rabbit polyclonal anti-KLF2	LifeSpan BioSciences	LS-B4570
Rabbit polyclonal anti-SGLT2/SLC5A2	Novus Biologicals	NBP1-91384
Mouse monoclonal TLR4	Novus Biologicals	IMG-5031-A, Clone#76B357.1
Mouse monoclonal anti-myeloperoxidase	R&D Systems	MAB3174, Clone# 392106
Bacterial and virus strains		
None used	NA	NA
Biological samples		
Human Aortic Tissue Microarray ($HIV^{+/-}$)	Tissue source South Africa	Email Lead contact: sxp579@case.edu
Human Aortic Tissue Microarray (Atherosclerotic/Healthy Controls)	www.biomax.us	# AR 301
Human Plasma Samples (HIV +/−)	Rustbelt CFAR Core D: Clinical Sciences. CWRU.	Contact PI/Project Leader: Jeffrey Jacobson jxj573@case.edu
Chemicals, peptides, and recombinant proteins		
2-NBD-Glucose (100μg/mL)	AbCam	#ab146200
Pam_3CSK_4 (10 ng/mL)	InvivoGen	tlrl-pms
Polyl:C (1μg/mL)	InvivoGen	tlrl-picw
Lipopolysaccharide/LPS (100 ng/mL)	InvivoGen	#LPS-B5:tlr-b5lps
Dapagliflozin (1μg/mL)	Cayman Chemical Co.	#11574
TLR-4 Inhibitor (TLR4-C34) (1μg/mL)	Cayman Chemical Co.	#18514
Imiquimod (1μg/mL)	InvivoGen	tlrl-imqs-1
CpG ODN2006 (500 ng/mL	InvivoGen	tlrl-2006g5
RNA later ™ Stabilization Solution	ThermoFisher Scientific	#AM7020
2-NBD-Glucose (100μg/mL)	AbCam	#ab146200
Critical commercial assays		
Human GM-CSF ELISA Kit	R&D Systems	#DY215-05
S-PLEX Human GM-CSF Kit (MSD)	Meso Scale Discovery	#K151F3S-1
EV Isolation Kit: ExoQuick® ULTRA	SBI System Bioscience	# EQULTRA-20A
Human TLR4 RNA Tissue Probe Set	ThermoFisher Scientific	# VA6-17278-VT
Human GM-CSF RNA Tissue Probe Set	ThermoFisher Scientific	# VA1-10275-VT
ViewRNA Tissue Assay Fluorescence Kits	ThermoFisher Scientific	# QVT0800
Slide Denaturation/Hybridization System	Biotang Inc.	#50-148-301
VECTASHIELD® Anifade Mounting Medium	Vector Laboratories	#H-1200-10
Chamber Slide System	Nunc™ Lab-Tek™ II	#154534
Chromium 3′ Gene Expression kit (v3.1)	10x Genomics	#CG000204
Deposited data		
Raw and Analyzed Data (Mendeley Data)	This Paper	"Mendeley Data: https://data.mendeley.com/datasets/rybh786pfh/2"

(*Continued on next page*)

Continued

REAGENT or RESOURCE	SOURCE	IDENTIFIER
Experimental models: cell lines		
Primary Human Aortic Endothelial Cells (Donor:81 y/M/Caucasian/Thoracic Aorta)	PromoCell	#C-12271, lot#473Z030.1
Experimental models: organisms/strains		
None used	NA	NA
Oligonucleotides		
Human TLR4 RNA Tissue Probe Set	ThermoFisher Scientific	# VA6-17278-VT
Human GM-CSF RNA Tissue Probe Set	ThermoFisher Scientific	# VA1-10275-VT
Recombinant DNA		
None used	NA	NA
Software and algorithms		
Microsoft Excel 2019	Microsoft Corporation	www.icrosoft.com
Prism 6.02 for Windows	GraphPad Software, Inc	www.graphpad.com
Fiji ImageJ, version 2.14.0.	Wane Rasband and contributors, NIH, USA	https://imagej.net/ij/
QuPath 0.4.4	QuPath developers, The University of Edinburgh	https://qupath.readthedocs.io/en/0.5/
Other		
None used	NA	NA

EXPERIMENTAL MODEL AND STUDY PARTICIPANT DETAILS

Study approval and ethics statement

The research involving human participants underwent a comprehensive review and received approval from both the University Hospitals of Cleveland and the University of the Witwatersrand in Johannesburg, South Africa. Sample collection and studies performed at the University of the Witwatersrand were approved by the University of the Witwatersrand Human Research Ethics Committee and Institutional Review Boards (IRB Protocol Ref. No: M130372). The 'Internal Review Boards,' of both universities approved the study and sample transfer plans in accordance with all applicable national and international regulatory standards. Prior to their involvement in this study, all patients and participants willingly provided written informed consent.

Study population and samples

Cells

The primary human aortic endothelial cell (EC) was purchased from PromoCell and cultured in glass slide chambers (Lab-Tek) with EGM-MV medium (PromoCell), according to the manufacturer's instructions. All experiments were performed using ECs between the 5th and 10th passages. ECs were treated with Escherichia coli lipopolysaccharide (LPS; L3024; Sigma Aldrich) at indicated time points and at a concentration of 100 ng/mL unless specified otherwise. At the end of treatment, ECs were immunostained and examined with fluorescence microscopy.

Plasma from healthy volunteers and PWH

Plasma samples from volunteer healthy controls and PWH were obtained from Rustbelt Sample Repository Core services: CFAR Core D at Case Western Reserve University (CWRU), Cleveland, OH.

Tissue preparation and constructing tissue microarray (TMA) paraffin block

Sample collection. This study was approved by the University of the Witwatersrand Human Research Ethics Committee. Arterial tissues from various major blood vessels were collected from 22 de-identified participants with 'documented peripheral vascular disease' – 12 without concomitant HIV infection and 10 with HIV infection (detailed in Table S1). Arterial tissue sampling was performed during arterial bypass grafting and were immediately transferred to RNAlater as per manufacturer's specified protocol and stored at −80°C. Following international shipping in dry-ice the samples were thawed, one part of the individual sample was washed in PBS and fixed in 10% buffered paraformaldehyde for 24 h, washed again in PBS and stored in 70% ethanol until histological processing and paraffin embedding and tissue microarray (TMA) slide preparation for future studies.

For additional studies, freshly cut de-identified human vascular TMA slides were purchased from US Biomax Inc.

Study design

The study employs a comprehensive methodology, utilizing techniques such as immunofluorescence microscopy, digital image data analyses, fluorescence *in situ* hybridization (FISH), enzyme-linked immunosorbent assay (ELISA), and statistical tests. The research includes quantitative assessments of GM-CSF, MPO, and TLR4 gene and protein expression in the endothelium, exploring the clinical and biological significance of TLR ligands and endothelium-derived GM-CSF. Both *ex vivo* and *in vivo* investigations were conducted to decipher the underlying mechanisms involved.

METHOD DETAILS

Single cell RNA sequencing (scRNAseq) and bioinformatics analysis

All analyses were conducted on EC samples, which were prepared following the 10x Genomics Fresh Human Adhered Cells Protocol. Single-cell RNA sequencing (scRNAseq) was performed on freshly detached early passage (passage number 3–7) ECs from the indicated treatments. The Applied Functional Genomics Core at CWRU utilized the 10X Genomics platform to generate single-cell indexed libraries. Approximately 10,000 cells were targeted per sample, and single cell libraries were generated using the 10x Genomics 3′ Gene Expression kit (v3.1) according to the manufacturer's protocol (10X Genomics). Following capture and lysis, cDNA was synthesized and amplified as per manufacturer's protocol (10X Genomics). Paired-end 100 cycle sequencing reactions were conducted on an NovaSeq S2 flow cell on an Illumina Novaseq 6000 platform, resulting in approximately 40,000 reads per cell. Illumina basecall files (*.bcl) were converted to FASTQs using CellRanger v3.0, which uses bcl2fastq v2.17.1.14. FASTQ files were then aligned to GRCh38 human reference genome and transcriptome using the CellRanger v3.0 software pipeline with default parameters; this demultiplexes the samples and generates a gene versus cell expression matrix based on the barcodes and assigns UMIs that enables determination of the individual cell from which the RNA molecule originated. Subsequently, Binary base call (bcl) files were converted to fastq format using Illumina's bcl2fastq2 software, and the data were then transferred to the Bioinformatics core for further analysis.

scRNAseq bioinformatic analysis

Bioinformatic analysis of cells based on whole transcriptomes was performed by the R package Seurat (version 4.3.0). Dimensionality of gene-barcode matrices was first reduced to 7 principal components using principal components analysis (PCA). PCA-reduced data were further reduced to 2-dimensional space using the UMAP method and visualized. Graph-based clustering of cells was conducted in the PCA space; a sparse nearest-neighbor graph of the cells was built first and Louvain modularity optimization was then applied. Differential gene expression analyses of each cluster were conducted by Wilcoxon rank-sum test. The log2 fold-change of a certain gene's expression (UMIs) in one cluster vs. all other clusters, and the corresponding adjusted *p*-values.

NBD glucose uptake assay

Early passages ECs were grown in chamber slides in EC medium. The assay the medium was changed with glucose free, phenol red free DMEM 24 h before the assay, and respective treatment reagents were added to individual chambers for overnight incubation. 2-NBD-Glucose was added to each chamber to a final concentration of 100μg/mL in glucose-free Phenol Red free DMEM 15 min before the end of the treatment time point on the day of experiment. After 15 min, the supernatants were aspirated, the slides were washed once in PBS and fixed in 4% paraformaldehyde for 10 min, followed by rinsing once PBS, dehydrated with graded ethanol 50% > 70% > 100%–1 min each, and air dried. Slides were then mounted in anti-bleach mounting medium (Vectashield) with DAPI and examined by an automated tabletop epifluorescence microscope (EVOSFL; Life Technologies).

ELISA

The GM-CSF levels in endothelial cell culture supernatant and in human plasma samples were quantified by using human GM-CSF Duo Set ELISA kit (R&D Systems, Cat# DY215-05). The high sensitivity MSD S-PLEX Human GM-CSF Kit (Meso Scale Discovery. Cat #K151F3S-1), was also used to repeat and confirm the plasma sample data (not shown). We also measured the lipopolysaccharide levels in plasma from healthy control and PWH using a high sensitivity Lipopolysaccharide ELISA Kit (LS Bio, Cat# LS-F17912-1). Kit specific protocols were stringently followed.

Detection of GM-CSF by western blotting

Protein concentrations were assessed using a NanoDrop2000 spectrophotometer in the following samples: endothelial cell (EC) lysate, EC medium supernatant collected at 72 h, and extracellular vesicles (EVs) obtained and purified from the respective EC medium using the ExoQuick TC EV Isolation Kit from SBI, following the manufacturer's recommended procedure. All protein-related procedures were carried out at 4°C in a lysis buffer supplemented with protease and phosphatase inhibitors. Following a brief centrifugation, the resulting supernatants were combined with an equal volume of an SDS-PAGE sample buffer containing DTT. Approximately 50 μg of protein was loaded onto a 10% Tris-HCl gradient gel and subsequently transferred to PVDF membranes for the immunodetection of human GM-CSF using an LI-COR system.

Fluorescence in situ hybridization

The FISH experiments for TLR4 and CSF2 RNA were performed using ISH Tissue Assay Fluorescent kit and respective probe sets (ThermoFisher Scientific) strictly according to the manufacturer's specified protocols. Briefly, the freshly cut TMA slide were baked at 60°C for 1 h, deparaffinized, rehydrated, and heat pretreated with 1X 'Pretreatment Solution' (provided in the kit) at 95°C for 25 min. After washing with PBS, the slides were digested with Protease QF 1:100 (provided in the kit) in prewarmed PBS and incubated at 40°C for 10 min. After removing excess PBS, the slides were refixed with 10% formaldehyde for 5 min at room temperature and washed twice in PBS. Before hybridization, the remaining liquid was decanted. Probes used: 1. Human GM-CSF RNA (*CSF2*) Tissue Probe Set, Type 1 (VA1-10275-VT, target region: Chr.5:132073792-132076170 on Build GRCh38, reference sequence: NM_000758.3). 2. Human *TLR4* RNA Tissue Probe Set, Type 6 (VA6-17278-VT, target region:Chr.9:117704175-117717491 on Build GRCh38, reference sequence: NM_003266.3, NM_138554.4, NM_138557.2). The respective probes were diluted 40-fold in Probe set diluent QT (provided in the kit) and applied to the slide, which was subsequently covered with a 24 × 50 mm^2 coverslip and sealed with rubber cement. The sealed slides were preheated at 85°C for 5 min and then hybridized at 40°C for 2 h in the slide ThermoBrite Denaturation/Hybridization System. Subsequent signal amplification fluorophore tagging was performed according to the provided assay manual. We also extended the FISH protocol to allow detection of *CSF2* RNA and GM-CSF protein by FISH sequential dual GM-CSF immunofluorescence staining of the same TMA slide following the manufacturer's protocols. Subsequently, the slides were mounted using Vectashield with DAPI antifade medium for microscopy.

Immunofluorescence labeling and microscopy

Tissue immunostaining

For immunohistochemical and immunofluorescence staining, tissue microarray (TMA) sections of blood vessels were baked at 60°C for 1 h, deparaffinized, rehydrated, fixed in 4% paraformaldehyde for 10 min, and processed at 95°C for 20 min in Citrate Epitope Retrieval buffer (10mM Sodium Citrate, 0.05% Tween 20, pH 6.0), followed by blocking with 2% bovine serum albumin in Tris-buffered saline plus Triton X-100 0.025% for 1 h at room temperature. The slides were then incubated overnight at 4°C with respective primary antibody in blocking buffer, at the manufacturer's recommended concentrations. Samples were washed and exposed to fluorescein isothiocyanate and/or rhodamine red–conjugated secondary antibodies (Jackson ImmunoResearch Laboratories).

Microscopy

The slides were mounted using Vectashield with DAPI anifade mounting medium and microscopy was done using an automated epifluorescence microscope (EVOSFL; Life Technologies). The fluorescent microscopic images of EC on chamber slides and TMA slides were taken by an epifluorescence microscopy (EVOSFL; Life Technologies) using ×20, ×40, and ×100 oil immersion objectives.

QUANTIFICATION AND STATISTICAL ANALYSIS

Quantification

We used the public domain software (ImageJ, version 2.14.0. http://ImageJ.nih.gov/ij/; and Q-Path, v0.4.4. https://qupath.github.io/) to process and analyze the digital image data.[50,51] Briefly, images of each fluorochrome channel were converted to 8-bit monochrome images, and the background value was subtracted to 0. In aortic tissue sections the endothelium and sub-endothelial regions were precisely selected the mean fluorescence intensity was recorded for respective color channels. The fluorescence intensity value measured for nuclear DAPI and other target signals using the same region of interest (GM-CSF, TLR4, KLF2, eNOS). In some analyses, we determined the target to nuclear fluorescence ratio (Fc/n) according to the formula Fc/n = (Fn − Fb)/(Fc −Fb), where Fb is background autofluorescence.[14,52] For GM-CSF and MPO protein expression, we presented the data as mean fluorescence intensity (MFI) values. To perform the data processing and statistical analyses, we used GraphPad Prism (v10.2), and Microsoft Excel software (Microsoft Office Professional Plus 2013).

Statistical analysis

Here is a summary of the statistical tests used for each analysis for this study which is mentioned in the respective figure legends. Values are expressed as means ± standard errors of mean (SEM). All statistical tests were performed in GraphPad Prism (v10.2.2), and/or Microsoft Excel 2016. We used the 2-tailed non-parametric Mann–Whitney U test to compare the independent group frequencies of sub endothelial inflammatory signals, and fluorescence intensity ratios. The correlation and multiple regression analyses were done using IBM-SPSS and GraphPad Prism (v10.2.2). We subsequently verified the results using IBM-SPSS software V29.0.1.0 (171). Differences were considered significant at $p < 0.05$. For relative mRNA and protein expression of specific markers, significance was tested using Mann Whitney U test when comparing two groups, and one way ANOVA for multiple comparison when comparing three groups. In the respective figure legends, N represents the number of individual tissue donors, number of images used, or number of cells of cells used in a specific experiment.